

Evaluating CT for Metrology: The Influence of Material Thickness on Measurements

Joseph SCHLECHT¹, Eric FERLEY¹, Shaun COUGHLIN¹, Steven D. PHILLIPS²,
Vincent D. LEE², Craig M. SHAKARJI²

¹North Star Imaging, Inc., Rogers, MN, USA, {jschlecht, eferley, scoughlin}@4nsi.com

²National Institute of Standards and Technology, Gaithersburg, MD, USA

Abstract

X-ray imaging provides a non-destructive means to measure internal features of an object, and computed tomography (CT) offers unique capabilities for internal measurements in 3-D. However, due to the computational nature of CT and its indirect measurement process, assessing its efficacy for metrology is essential. CT reconstruction artefacts are of primary concern as they may influence measurements. In this paper we investigate the effect of varying material thickness on CT reconstructions for metrology. We show that applying varying thicknesses of the same material as the object being measured does not present significant issues for CT-based metrology. The results advocate further exploration of CT as a means for internal object measurement and metrology.

Keywords: Computed tomography (CT), metrology, CT reconstruction artefacts, material thickness

1. Introduction

We present an evaluation of computed tomography (CT) as a means for metrology when an object of interest has varying material thickness. As an x-ray beam passes through material, its spectra may change, or harden, and create undesirable artefacts in the reconstruction. These artefacts can create errors in subsequent dimensional measurements of the object based on CT data. For example, an object of a uniform material may appear to have non-uniform density, which can impact CT reconstruction by negatively influencing surface detection and localization. Our goal in this paper is to evaluate whether effects from material thickness introduce significant bias into dimensional measurements.

There are many possible sources of CT reconstruction artefacts. We focus here on those from varying material thickness and their impact, if any, on metrology. We aim to establish whether artefacts from material thickness could rule out the use of CT for metrology applications. If varying material thickness in an object is significantly detrimental to measurement accuracy, we would be unable to place reasonable error bounds on measurements, making it inappropriate to use CT for metrology.

Determining whether material thickness is an issue for CT and metrology is fundamental and timely research. Metrology is already a well established field, particularly as it relates to tactile and optical coordinate measuring machines (CMMs). While industry accepted standards have defined procedures for quantifying and qualifying measurements from CMMs [3, 4], CT for metrology is still developing formal standards. Currently there is a lack of international standards accepted by all CT manufacturers. Hence there are fundamental questions that still need to be answered and investigated, such as material thickness effects on measurements.

International consensus for CT and metrology standardization is currently a work in progress. Some CT manufacturers marketing machines for metrology have announced adoption of the VDI/VDE 2617 and 2630 specifications [8, 9], which attempt to apply the ISO 10360 standards for use with CT. Currently, there is an ISO working group to standardize CT for use with

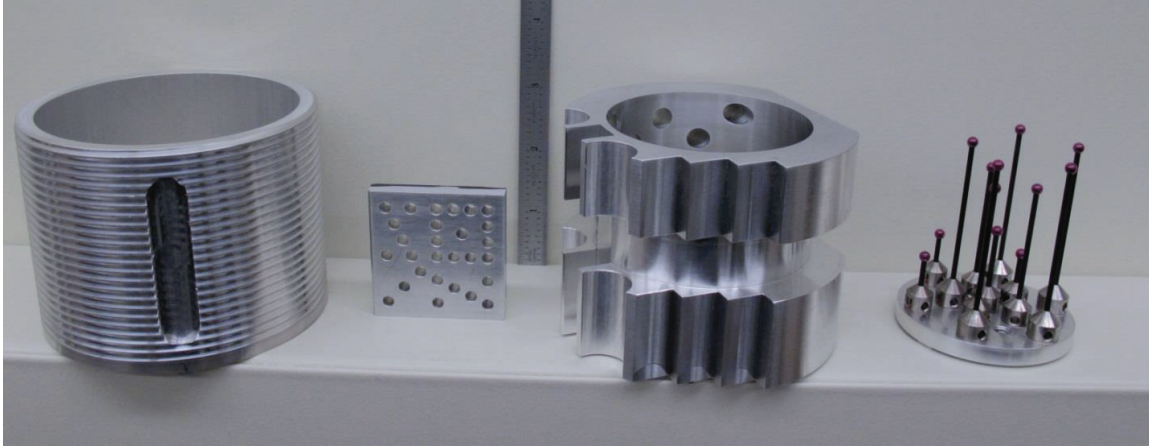


Figure 1: From left, the thread shell, hole plate, gear shell, and styli forest. All are aluminum except the styli forest, which has aluminum oxide (ruby) balls on carbon fiber stems. The hole plate and styli forest were CT scanned and measured with and without each shell around them.

metrology [2]. However, publication and adoption of this standard lie several years into the future.

A recent CT audit for metrology found that most participants were unable to appropriately report measurement uncertainty of the system they used [1]. This poses a serious challenge for a rigorous treatment of metrology in CT systems on a basic level and underlines the idea that CT for metrology is a developing area with fundamental questions that still need to be answered. From this perspective, our work is just one in a series that should evaluate whether it is appropriate and justified to use CT for metrology.

The results presented here were investigated in support of the ISO TC213/WG10 standards development effort [7]. Similar results were reported in another WG10 report from a group at the University of Padova [5], where they compared length measurement errors from the same hole plate used here with an added 10 millimeter aluminum block. They concluded that the extra material did not visibly impact measurements. A similar WG10 report from a group at the University of North Carolina Charlotte found that material variation might not cause large measurement error [6]. They note, however, that beam hardening correction algorithms play an important role, and that it is important to choose good parameters for such a correction.

In the following sections we describe our experimental design to determine the influence of material thickness on measurements, including our reference objects and acquisition procedures. This is followed by experiment results and a few conclusions.

2. Design of experiments

Our goal is to evaluate the influence of varying material thickness on measurements from CT data. We attempt to do so by scanning two reference objects with and without additional material placed in the x-ray beam path. We assume a knowledgeable and experienced operator that is able to choose appropriate measurement configurations that would normally be available on a CT system, including x-ray technique, physical filters, and beam hardening correction factors.

To evaluate material influence, the reference objects were scanned with two types of “shells” placed around them. Figure 1 shows images of the objects and shells. One object was an aluminum hole plate produced by NIST based on a design by the Physikalisch-Technische Bundesanstalt (PTB), the other was a “styli forest” comprising carbon fiber rods and ruby spheres

CT Parameter	Value
Detector size	1536 × 1920 pixels
Pixel pitch	127 μm
Integration time	250 ms
Frame averaging	6 frames / image
Projections	1800 images
Source-to-detector	480.179 mm
Source-to-object	155.822 mm
Magnification	3.08
Optimal voxel size	41.23 μm
Physical filter	Cu 2.286 mm
X-ray voltage	220 kV
No shell current	170 μA
Thread shell current	190 μA
Gear shell current	200 μA

Table 1: Technique parameters and values for CT scans of the hole plate and styli forest. All parameter values remained the same for every scan except x-ray current, which was modified for each shell configuration.

produced by NIST. The hole plate lends itself to uni- and bi-directional measurements with material of varying thickness between the holes. In contrast, the styli forest does not contain material between its spheres, and all measurements were uni-directional between ball centers.

The two shells that were placed around the objects are made of aluminum and produced by NIST. They contain a high variation of material thickness and are useful to test whether adding material of varying thickness significantly influences measurement results. The thread shell has a wall thickness of 6.4 mm and includes an externally threaded surface with 8 threads per inch. The gear shell has a wall thickness of 15 mm with large features that are 12.5 mm deep. Both shells also include several holes and slots to further present material thickness variation.

The hole plate and styli forest were each scanned three times without shells. This was done to establish a mean value for the measurements (reducing random effects) and to determine the variation in three measurements. Since we are looking for systematic effects between the shell-on and shell-off measurements, these objects are not calibrated and the mean shell-off measurement result was used to determine the nominal values. After the first scan without a shell, two scans with the gear shell were acquired. This was followed by a second shell-off scan and two scans using the thread shell. A third and final shell-off scan was then acquired. The shells were positioned in the same way over the objects during both scans to rule out any potential bias from shell orientation.

Techniques that compensate for varying material thickness were used. The idea was to use all available techniques that a knowledgeable and experienced user of a CT system has access to. If different techniques were needed to produce a higher quality reconstruction when the shells were in place, then they were used. The intention was to obtain the best quality data possible, assuming all techniques typically available to a knowledgeable and experienced user.

The techniques chosen for acquisition of the hole plate and styli forest were the same. For the no shell, thread shell, and gear shell scans the only difference was a modified x-ray current. Table 1 details the technique for x-ray source, detector, and other parameters.

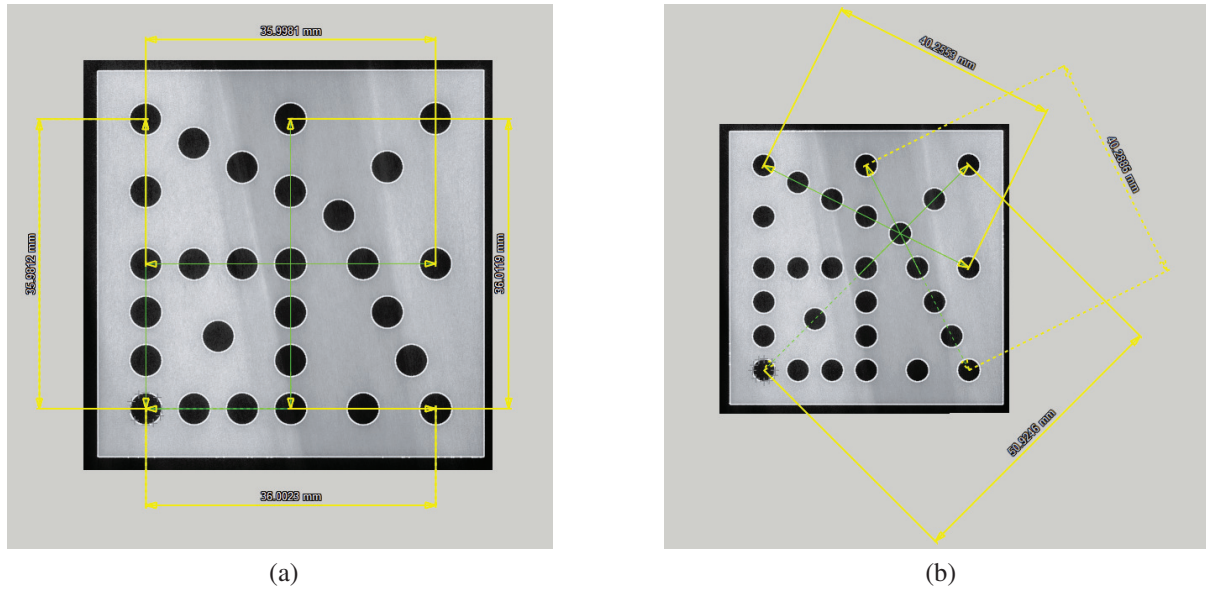


Figure 2: Hole plate measurement directions, as suggested by ISO TC213/WG10. The green lines in (a) show two horizontal and two vertical directions, and in (b) two angled and one diagonal direction. Six holes were used in each direction to make five measurements of increasing length. Uni- and bi-directional measurements were made between holes. Best viewed in color.

2.1 Hole plate description

The aluminum hole plate was obtained from NIST and has a dimension of $48 \text{ mm} \times 48 \text{ mm} \times 8 \text{ mm}$. Figure 2 describes the layout of the 28 holes, each with a nominal diameter of 4 mm. The holes are arranged in horizontal, vertical, and angled series in order to provide multiple length measurements over several directions in the reconstructed volume.

Hole plate measurement procedures and nomenclature from ISO TC213/WG10 were used to obtain a systematic set of uni- and bi-directional measurements. For each direction of six holes, the first in the series was selected to serve as the zero point for the length measurements along that line. Five measurements of increasing length were then made from the first hole to the others in the same direction. This was done to obtain a series of five increasing length measurements in the horizontal, vertical and angled directions.

Figure 2 shows seven series of measurements made in various directions. They include two horizontal (H series), two vertical (V series), two at an off-diagonal (A series), and one set of diagonal (D series) measurements. For each scan, there was a total of 35 uni- and 35 bi-directional measurements.

The uni-directional measurements give the distance between two hole axes at the plate mid-plane. The bi-directional length between two holes is defined as the uni-directional length plus the distance from each hole center to the hole edge along the uni-directional measurement line.

2.2 Styli forest description

The styli forest was produced by NIST and comprises 12 aluminum oxide (ruby) balls on carbon fiber stems. The ruby balls have a nominal diameter of 4 mm. The stylis are uniformly distributed on the xy -plane as in Figure 3a. Their height is distributed among four different elevations, illustrated in Figure 3b and detailed in Figure 3c.

Uni-directional measurements are made between the center-to-center distance of each pair

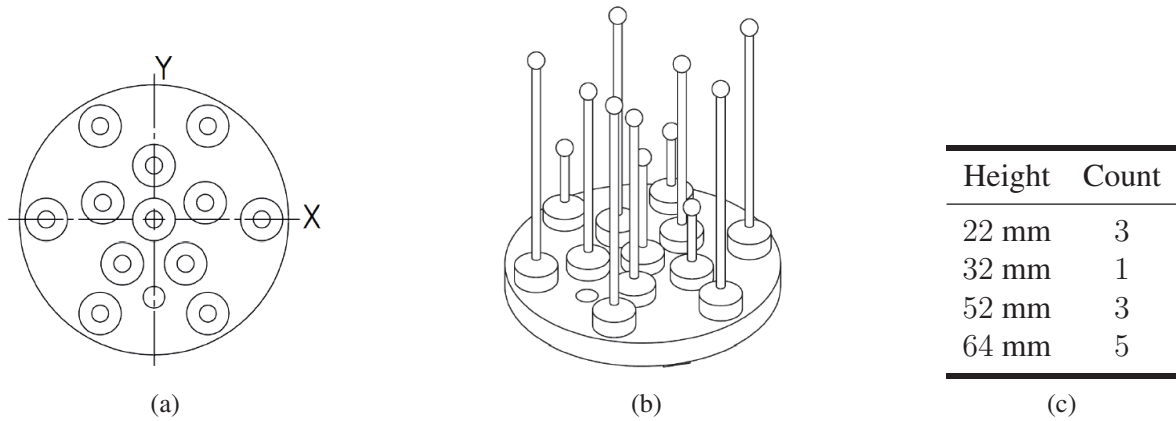


Figure 3: Styli forest layout. (a) The stylis are uniformly distributed on the xy -plane, and (b) their height is distributed among four different elevations. (c) Styli forest height distribution.

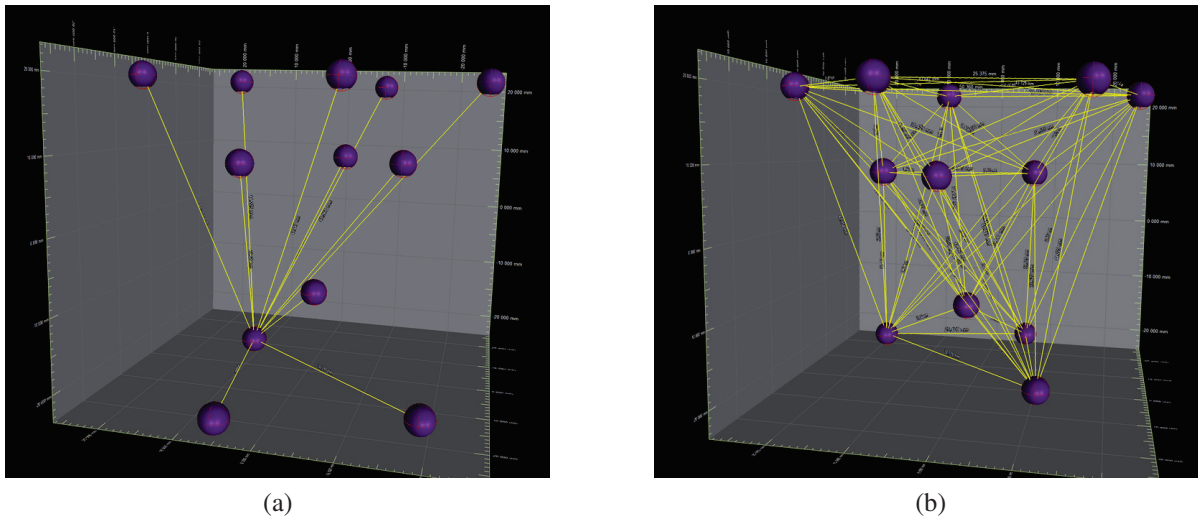


Figure 4: Styli forest measurements. The yellow lines in (a) show 11 measurements from one ball to all others, and in (b) 66 measured lengths from each ball to all others. Only uni-directional measurements from sphere centers were made.

of balls, for a total of 66 measurements. In this way there are measurements of various length across different heights. Furthermore, the measurements are made in many directions of the reconstruction volume, revealing if there is a bias in a particular direction. Figure 4 shows examples of fit spheres and the measurements made between sphere pairs.

3. Results

As previously described, results are reported for each reference object with and without shells. Since we are looking for systematic effects between the shell on and shell off cases the objects are not calibrated. To reduce random effects, three scans without shells are combined to produce mean measurement results, which are then used as nominal values. Measurements made with the shells around the reference objects are then compared against the nominal values.

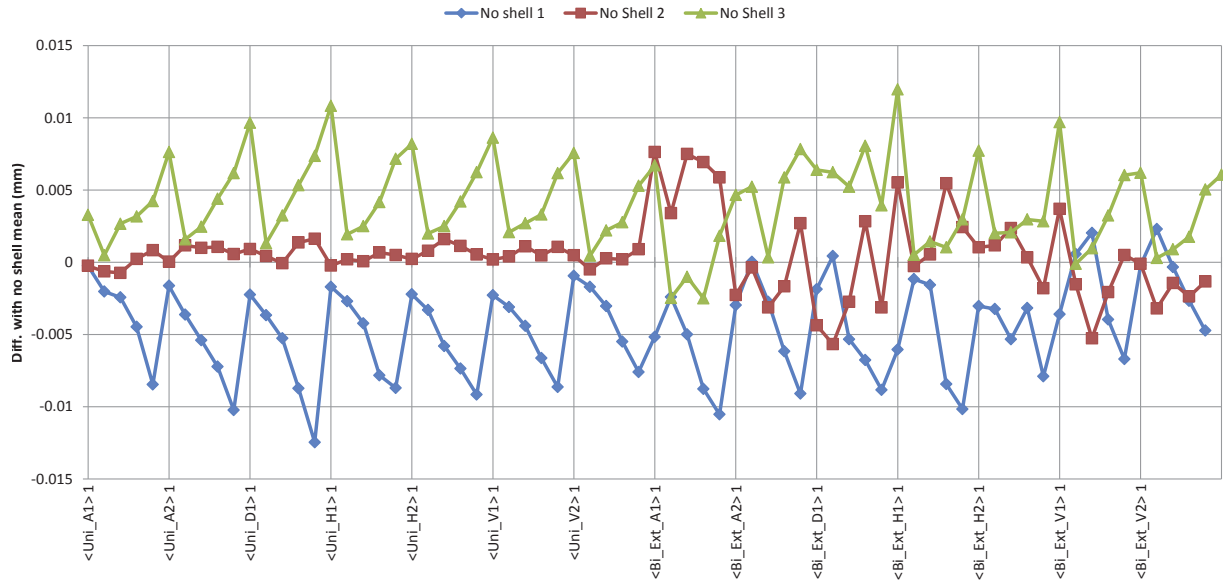


Figure 5: Hole plate measurements for three CT scans with no shell. Uni- (“Uni_”) and bi-directional (“Bi_Ext_”) results are given as a difference with the mean. The TC213/WG10 hole plate nomenclature is used to indicate direction and the five increasing-lengths per direction (A=angle, D=diagonal, H=horizontal, V=vertical).

3.1 Hole plate

Figure 5 shows the difference from the mean of three sets of uni- and bi-directional measurements scanned without shells. We observe that more than 97% of the 210 measurements are within $10\ \mu\text{m}$ of their mean. It is also clear from these plots that the uni-directional measurements show regularity in their error, based on increasing length. In the bi-directional case the distribution of error is more random, which is expected due to bi-directional measurements being more susceptible to error from detecting the surface of the holes.

In Figure 6 we show two sets of measurements using the gear and thread shells subtracted from the no shell mean. We see that there is less error relative to the no shell mean in the uni-directional case than the bi-directional case. Further, 90% of uni-directional measurements are within $5\ \mu\text{m}$ of the no shell mean. For bi-directional measurements, 92% are within $10\ \mu\text{m}$ of the mean. In both cases, the error is within the deviation of the no shell measurements.

3.2 Styli forest

Figure 7 shows measurement differences from three styli forest scans without shells compared to their mean. As with uni-directional measurements of the hole plate, the styli forest deviations increase with measurement length. We also observe that more than 97% of the measurements are within $10\ \mu\text{m}$ of their mean.

By placing the shells around the styli forest and taking the difference of measurements from the no shell case, we obtain the gear and thread results in Figure 7. We see that the deviations are within the measurement variation observed in the no shell scans. Further, all measurement differences are less than $10\ \mu\text{m}$ from the mean of the no shell case, and over 90% are within $7\ \mu\text{m}$.

Of further interest is the strong linear fit the measurements follow. Also note that the decreasing slope of the fit follows the order in which the scans were acquired. The residuals of a linear regression to each of the gear and thread shell cases are given in Figure 8. The plot

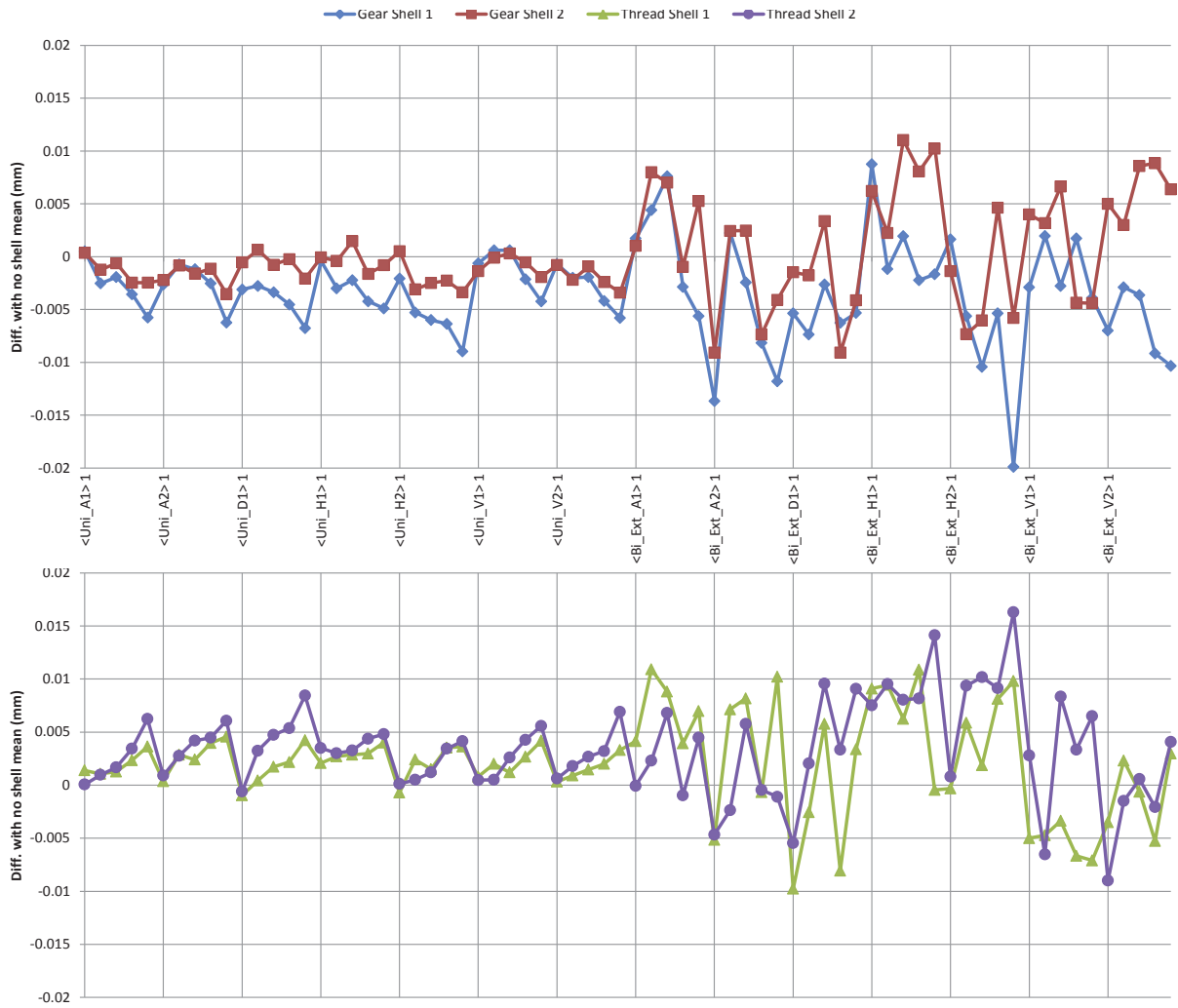


Figure 6: Hole plate measurements for CT scans with the gear shell (top) and thread shell (bottom). Uni- and bi-directional results are given as a difference with the mean of three no shell scans.

shows that nearly 90% of measurements with shells are within $1 \mu\text{m}$ of a fit line. Both the linear dependence of the deviations within a series, and the time-ordered dependence between series strongly argue that a progressive, uncorrected thermal expansion due to heating occurred.

Figure 9a shows the error of the estimated styli forest ball diameter. The diameter error is given as a difference with the nominal ball size of 4 mm. We see that as the stylus height increases, so too does the error compared to the nominal diameter. This is due to cone beam CT artefacts, which cause the balls to be misshapen based on a surface fit. The diameter error with respect to the no shell mean is given in Figure 9b, which shows that adding extra material resulted in $2 \mu\text{m}$ of variation.

The form error of the styli balls (min-max) is given in Figure 10a. Here, too, it is clear that as the styli height increases, the form error does as well. This is also caused by cone beam CT artefacts. Moreover, it is interesting to see that the form error is smallest closest to the center of the beam vertically (near 32 mm). Figure 10b shows the form error as a difference with the mean no shell case, which is typically less than $6 \mu\text{m}$. We note that the form error is more sensitive to cone beam CT artefacts due to its calculation based on extreme values, whereas the diameter is based on a least square fit to the surface points of a ball.

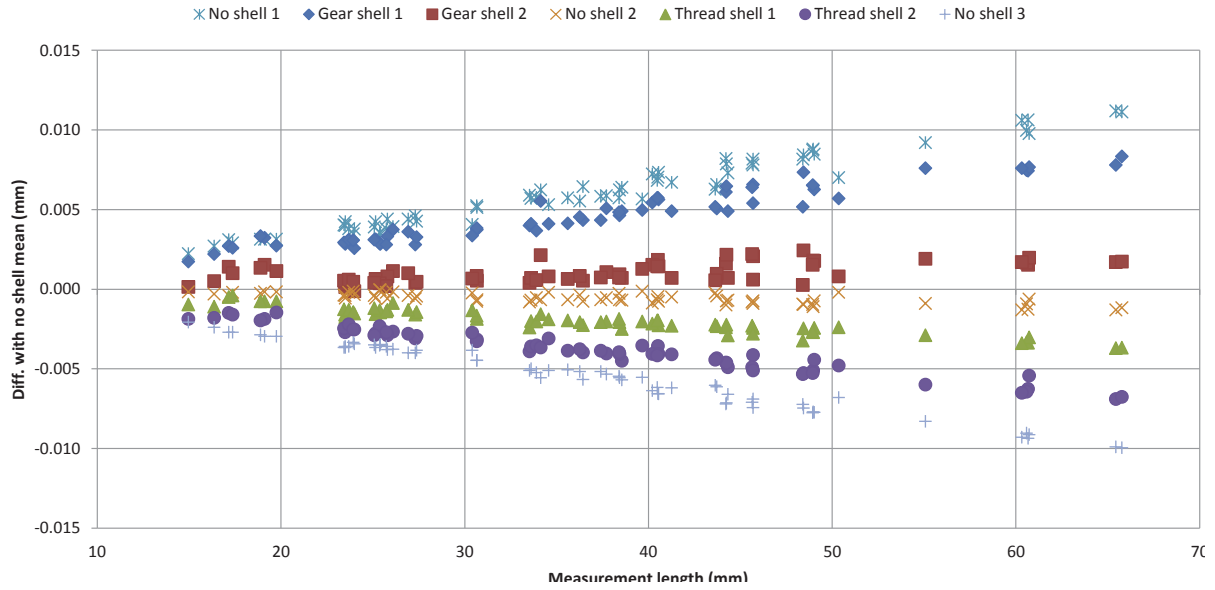


Figure 7: Styli forest measurements for CT scans with and without shells. Uni-directional measurements were made from center-to-center of each pair of spheres. Results are given as a difference with the mean of the three no shell scans.

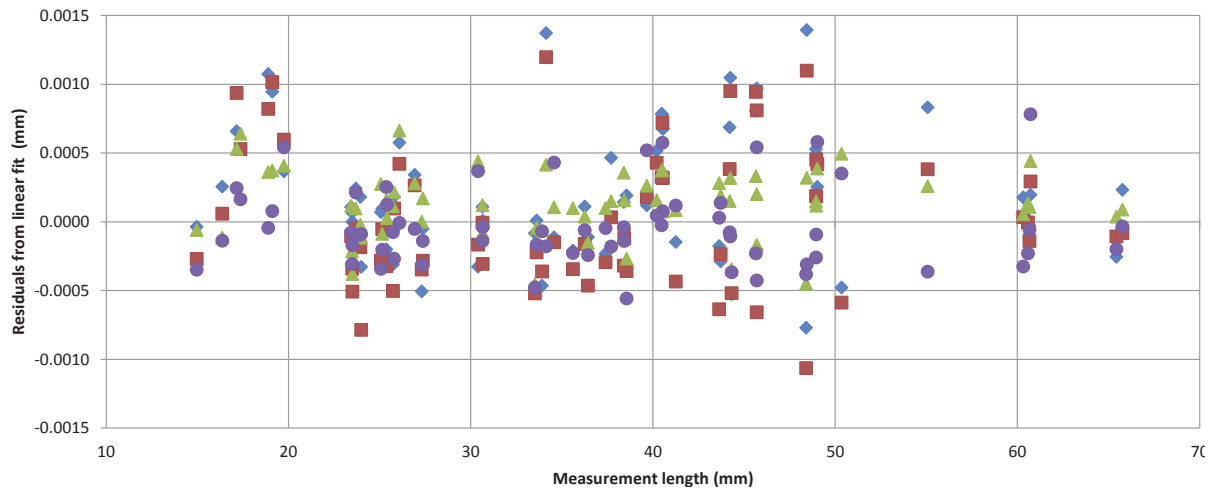


Figure 8: Residual error from a linear fit to each series of gear and thread shell measurements in the styli forest (see fig. 7).

4. Conclusions

To determine whether varying material thickness is an issue for CT and metrology, we compared measurements with shells of varying thickness against the mean of measurements without a shell. Without a formal uncertainty budget, it is difficult to precisely determine whether the effect of material thickness is completely inconsequential. However, we can determine from the results whether the error caused by varying material thickness exceeds the range of variation observed when no extra material is added.

The results indicate that when shells are added to both reference objects, more than 90% of uni-directional measurements are within $7 \mu\text{m}$ of the no shell mean, and over 90% of bi-directional measurements are within $10 \mu\text{m}$ of the no shell mean. The differences observed when adding both the thread and gear shells fall within the range of deviations observed for

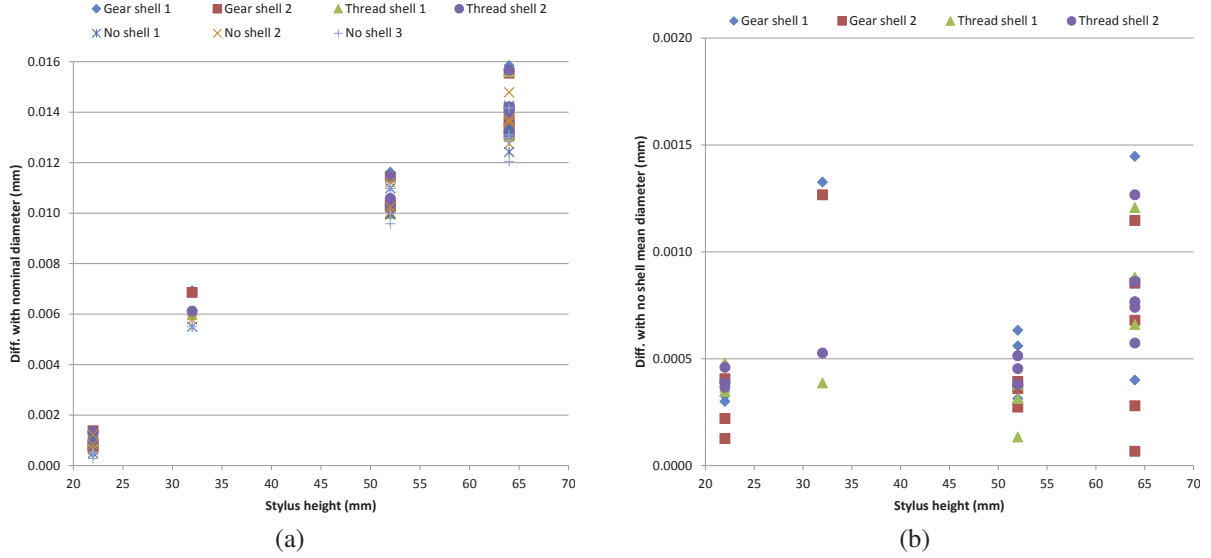


Figure 9: Styli forest diameter measurements with and without shells. Shown as (a) the difference with the nominal diameter (4 mm) and (b) the difference with the no shell mean diameter.

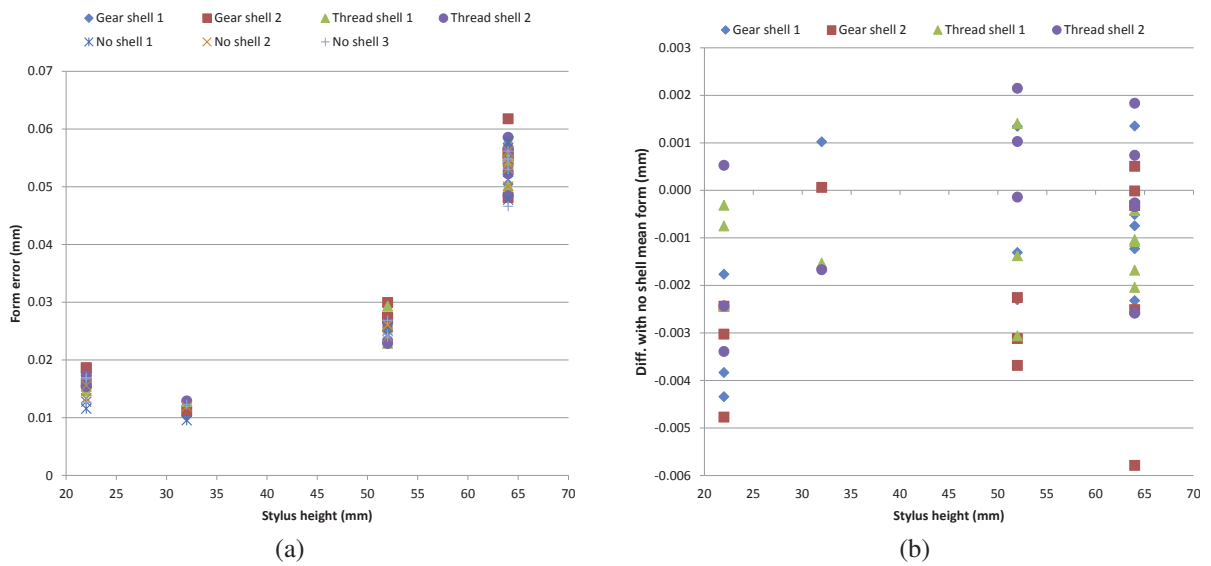


Figure 10: Styli forest form error of the least squares sphere fit with and without shells. Shown as (a) the form error for all scans and (b) the difference with the no shell mean form error.

the no shell mean. We conclude from these results that the measurement error from varying thickness of material is not significant. We further conclude that the magnitude of error is within published maximum permissible errors of some current CT systems marketed for metrology.

Additionally, the results show indications of thermal drift occurring during the measurements. The magnitude of this drift is larger than any indication of systematic bias due to thickness variations. Linear regression, which is equivalent to thermal expansion correction, fit 90% of the styli forest measurements to within 1 μm . This evidence strongly suggests that the dispersion between these series is caused by thermal drift and not material effects.

We also see from the results that the measurements are influenced by cone beam artefacts, as evidenced by the form and diameter errors of increasing stylus height. The balls in the styli

forest can be misshapen and create non-spherical surfaces due to missing surface information from the tops of the spheres throughout all views of the scan. These types of error could be significantly reduced by helical cone beam CT scans.

While it is informative to relate measurement error to real world units, relating errors to voxel size could also be useful. CT systems have a pixel and voxel budget available for imaging an object. Based on characteristics of physical detectors and magnification level, there is a limited number of pixels that can be inside an object. Tactile CMMs are not limited in this way, but optical CMMs also have a pixel budget, which is reflected in their relatively large maximum permissible errors compared to tactile CMMs. For a given level of magnification in a CT system, measurement error should scale up as magnification decreases and fewer voxels cover the object.

Expressing measurement error as a factor of voxel size generalizes it beyond a single level of magnification. Measurement error less than the optimal voxel size is significantly impacted by error in pixel gray values. For example, noise, scintillation material, and fill factor all contribute to inaccurate pixel values and measurement error. Relating our results to voxels, we see that the uni-directional errors are 17% of the optimal voxel size, and in the bi-directional case 24% of a voxel. A maximum permissible error statement does not generalize over multiple levels of magnification, even though the relationship may exist.

Disclaimer: Materials may be identified in order to adequately specify certain procedures. In no case does such identification imply recommendation or endorsement by the National Institute of Standards and Technology, nor does it imply that the materials identified are necessarily the best available for the purpose.

References

- [1] S. Carmignato, A. Pierobon, and E. Savio. Interlaboratory comparison of computed tomography systems for dimensional metrology. Technical report, University of Padova, 2011.
- [2] ISO10360-11:2009 (Working Draft). Geometrical product specifications (GPS) – Acceptance and reverification tests for coordinate measuring machines (CMM) – Part 11: CMMs using the principle of computed tomography (CT). Under development.
- [3] ISO10360-2:2009. Geometrical product specifications (GPS) – Acceptance and reverification tests for coordinate measuring machines (CMM)– Part 2: CMMs used for measuring linear dimensions. *International Organization for Standardization*, 2009.
- [4] ISO10360-8:2009. Geometrical product specifications (GPS) – Acceptance and reverification tests for coordinate measuring machines (CMM) – Part 8: CMMs with optical distance sensors. *International Organization for Standardization*, 2013.
- [5] ISO/TC 213 WG10. Experimental study on material influence in dimensional computed tomography. Filippo Zanini and Manuel Balcon and Simone Carmignato, Jan 2014.
- [6] ISO/TC 213 WG10. Preliminary report from UNC Charlotte on CT measurements of hole plates. University of North Carolina, Charlotte, Jan 2014.
- [7] ISO/TC 213 WG10. Preliminary report on material influence in dimensional computed tomography. North Star Imaging, Inc. and National Institute of Standards and Technology, Jan 2014.
- [8] VDI/VDE. 2617 Part 13: Accuracy of coordinate measuring machines – Characteristics and their testing - Guideline for the application of DIN EN ISO 10360 for coordinate measuring machines with CT-sensors. 2011.
- [9] VDI/VDE. 2630 Part 1.3: Computed tomography in dimensional measurement – Guideline for the application of DIN EN ISO 10360 for coordinate measuring machines with CT-sensors. 2011.